

STRENGTHENING MECHANISM OF GRAPHENE/METAL NANOLAYERED COMPOSITES

Zhenyu Yang, Dandan Wang, Jian Sun and Zixing Lu

Institute of Solid Mechanics, School of Aeronautics Sciences and Engineering,
Beihang University, XueYuan Road No. 37, HaiDian District, Beijing 100191, China
Email: zyyang@buaa.edu.cn, Web Page: <http://www.ase.buaa.edu.cn/szdw/fxqjgqdx/63397.htm>

Keywords: graphene, toughness, dislocation, nanolayered composites, molecular dynamics

Abstract

In recent years, graphene/metal nanolayered composites have been synthesized with superior mechanical properties. Experiments showed that the strength and hardness of metals can be dramatically enhanced with ultra-low volume fractions of graphene inclusions, but a fundamental understanding of deformation mechanism of the nanolayered composites is lacking. Molecular dynamics simulation was employed to investigate the deformation mechanisms of graphene/metal nanowires with layered structures. The results show that the strengthening mechanism of nanolayered graphene/metal nanowires depends on the necessary stress for dislocation nucleation and also the surface morphologies. Graphene can be used as an effective barrier against dislocation motion in nanolayered composites. The present results are expected to contribute to the design of novel metal matrix nanocomposites enhanced by graphene.

1. Introduction

Graphene exhibits excellent mechanical, electrical and thermal properties [1-3], which attracts great attention and intensive study in applied physics and material science. In particular, graphene is specified by both superior tensile strength of about 130 GPa and Young modulus of about 1 TPa [3], and the extreme surface-to-volume ration, which make it possible to be an ideal reinforcement for nanocomposites [4]. Over the past decade, researchers have successfully synthesized graphene-based nanocomposites with metal-matrix, which exhibits superior mechanical properties with great potential applications in nanotechnology [5-7]. In particular, an important progress was made by Kim et al. [8], who recently successfully fabricated Cu- and Ni- matrices nanolayered composites reinforced by only single layers of graphene. The experiments [8,9] showed that the strength and toughness of graphene/metal nanolayered composites can be highly enhanced, with ultra-high strengths of 1.5 GPa and 4.0 GPa for graphene/Cu and graphene/Ni, respectively. These values are the highest for ever fabricated graphene/metal composites.

Chang et al. [10] studied full atomistic simulations on nanoindentation of Ni-graphene nanocomposites with varied numbers of graphene layers. The results showed that as the number of graphene layers increases, the hardness of the nanocomposites decreases, but the maximum elastic deformation of graphene/Ni nanocomposites increases. Liu et al. [11] studied the strengthening effects of graphene-metal nanolayered composites under shock loading with using molecular dynamic simulation. They found the strong sp²-bonded structures of graphene constrain the dislocations and heal the materials. Ovid'ko et al. [12] theoretically studied that competition between plastic deformation and fracture processes in graphene-metal nanolayered composites. They found the

strength of graphene-metal nanolayered composites as functions of the key structural parameters, including the metallic layer thickness and graphene layer thickness. Huang et al. [13] analyzed the radiation damage resistance of graphene/Cu nanolayered composite and found the damage may impair interface stability and then weaken the radiation damage resistance of the composite.

Different from the randomly distributed graphene composite, graphene is distributed flatly with equal layer spacing at axial direction in the graphene/metal nanolayered composite, which shows similar periodic nanostructure with the metallic multilayers [14,15]. Atomic structure of the interface in metallic multilayers plays an important role in the dislocation core spreading and trapping in the interface plane [15]. But the graphene-metal interface could make a difference because the weak bending stiffness and strong in-plane structure of graphene [11]. As far as we know, most of the previous researches have been focused on graphene/polymer nanocomposites, and only a few attempts have been concerned with graphene/metal nanocomposites, especially the nanolayered composites. Graphene/metal nanocomposites with low volume fractions of graphene inclusions exhibit dramatically enhanced strength and hardness, but a fundamental understanding of deformation mechanism under mechanical loading is lacking, which is a prerequisite for design and application of this novel nanocomposites.

In this work, the emphasis is focused on the compressive behaviors of the graphene/Ni nanolayered composite nanowires using the molecular dynamics (MD) simulations. The dependence of the strength of composite nanowires on interlayer distance and surface morphologies is investigated with analysis of mechanisms of the dislocations blocking at interface and dislocations pile-up in a single layer. Our findings could be helpful to further understand strengthening mechanisms of graphene/Ni nanolayered composites.

2. Model and method

Based on the experiments [8], the configurations of the graphene/Ni nanowires are built as shown in Figure 1, in which four layers of graphene sheets are uniformly embedded into single-crystalline Ni [111] nanowires, since the (111) planes are the energetically favourable planes for plastic deformation in face centered cubic (FCC) Ni and the binding energy between graphene and metal is the highest on (111) surface [16]. Periodic boundary condition is applied along axial direction to eliminate the end effect. The lateral dimension of the SCS nanowire is about 8 nm, and the distance between neighbouring graphene sheets varies from 1.2 nm to 12 nm. Nanowires with two different cross-sections are both considered in presented work, as shown in Figure 1.

All the MD simulations in this paper are performed with using the large-scale atomic molecular massively parallel simulator (LAMMPS) [17], with combination of embedded atom method (EAM) [18] potential, reactive empirical bonding order (REBO) [19] potential and Lennard-Jones (LJ) potential together, which has been proved to be able to depict the two-type-atom system well [10]. The potential of LJ which describe the van der Waal's interaction can be given by the equation

$$U_{ij} = 4\varepsilon_{ij} \left[\left(\frac{\sigma_{ij}}{r_{ij}} \right)^{12} - \left(\frac{\sigma_{ij}}{r_{ij}} \right)^6 \right] \quad (1)$$

Where U_{ij} is a pair potential energy between the atom i and j . ε_{ij} and σ_{ij} are the coefficient of well-depth energy and equilibrium distance, respectively. Here $\varepsilon_{\text{Ni-C}} = 0.023049$ eV and $\sigma_{\text{Ni-C}} = 2.852$ Å [20] are adopted for all simulations.

Before loading, the models are first relaxed using the conjugate gradient method and then equilibrated at specified temperature using the Nose-Hoover thermostat [21] for 500 ps with NPT ensemble, in order to achieve stress free state in the axial direction. To compress the nanowires, the axial dimension is decreased at a constant rate of 10^8 /s at NVT ensemble. The equations of motion are integrated using

the Verlet leapfrog method [22] with a time step of 1 fs. The stress component is calculated using the Virial theorem [23]. The snapshots of the MD results are processed by the package of Atomeye [24].

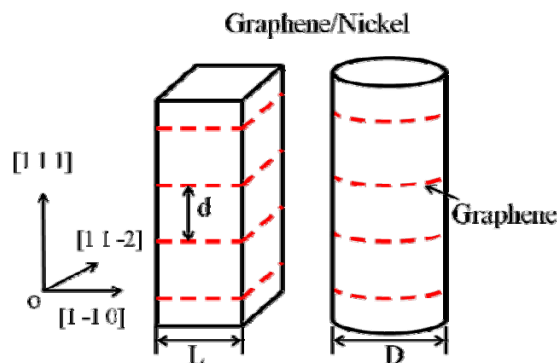


Figure 1. Illustration of the graphene/Ni nanolayered composite nanowire models with square cross-section (SCS) and circular cross-section (CCS). d for the distance between neighboring graphene sheets. $L = \sqrt{\pi}/2 D$ to keep the SCS nanowire and the CCS nanowire have the same cross-section area.

3. Results and discussions

3.1 Size-dependent yield stress

For comparison, the SCS nanowires and CCS nanowires are created with the same interlayer distance d and the same cross-section area. Figure 2 shows that the yield stress of graphene/Ni nanolayered composite nanowires changes with the interlayer spacing varying from 1.2 nm to 12 nm at the temperature of 10 K. The picture shows that the yield stress of the SCS composite nanowires is dependent on the interlayer distance between graphene sheets, but no obvious size dependence is found for the yield stress of CCS nanowires. For SCS nanowires, the stress for dislocation nucleation is low, and additional stress is necessary for dislocation to break the blocking by graphene. But for CCS nanowires, the stress for dislocation nucleation is high enough to lead nanowires yielding. As a consequence, no obvious contribution is made by the presence of graphene layers in CCS composite nanowires. The calculation results suggest that the strengthening mechanism depends on the necessary stress for dislocation nucleation and also the surface morphologies. Similar phenomenon was also found in nano-twined FCC metal nanowires with both square and circular cross-sections [25].

Figure 2 indicates that the relationship between the yield stress of SCS nanowires and interlayer spacing d can be fitted by Hall-patch relationship [26, 27]. For the SCS nanowires, the strength is tunable by control the interlayer distance between neighboring graphene sheets. That means the strength of SCS nanowires can be enhanced by decreasing the interlayer distance d , which has been proved by experiments [8]. The metal layers in simulations are all defect-free, but in experiments they always have pre-existed defects, which lower the stress for dislocation nucleation as well. That is why the contribution of graphene to strengthening is dominated in the graphene/metal nanolayered composites in experimental tests.

The typical stress-strain relationships of the SCS nanowire and CCS nanowire with interlayer distance $d=6$ nm are presented in Figure 3. This figure shows that the deformation of SCS nanowire is characterized by three dominant regimes: elastic, strain-hardening and strain-softening. The CCS nanowire yields at stress of about 30 GPa and deforms linearly until yielding. It is found in Figure 3 that no strain-hardening occurs in CCS nanolayered nanowires. However, the compressive stress-strain curves clearly show that in the SCS nanolayered nanowire, significant strain-hardening is enabled as the stress continues to increase after the yield point. In the following section, further evidence is

provided to confirm that the strength mechanism is that the nucleated partial dislocation blocked by graphene sheet.

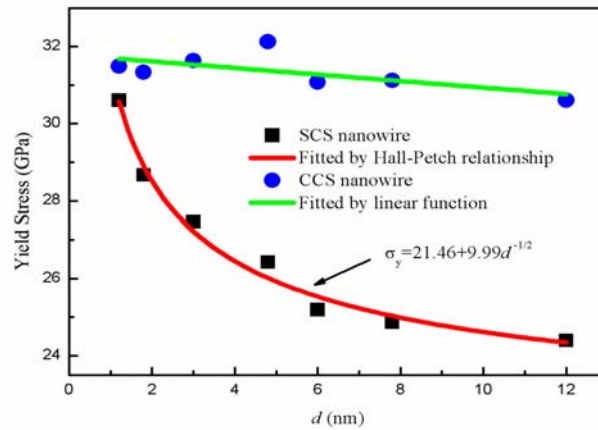


Figure 2. The yield stress of graphene/Ni nanolayered composite nanowires as a function of interlayer distance d .

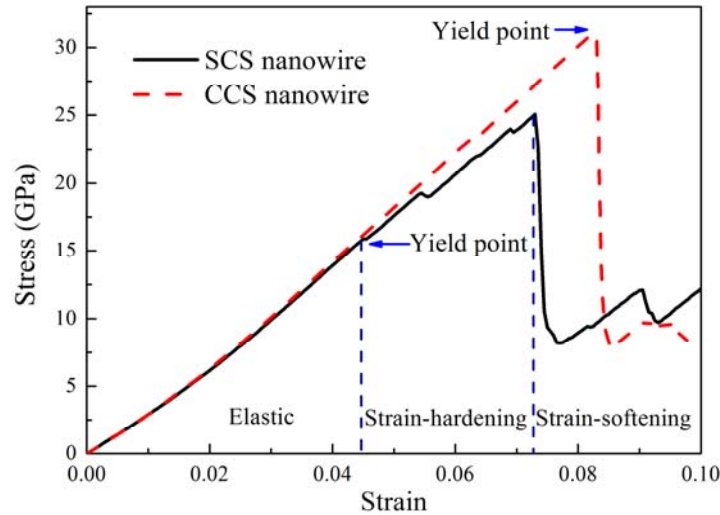


Figure 3. Comparison of typical stress-strain curves between SCS nanowire and CSC nanowire at temperature of 10 K.

3.2 Strengthening mechanism by graphene-metal interface

To understand the plastic deformation mechanisms, a dynamical observation of the typical dislocation activities during the initial yielding deformation of SCS nanolayered nanowire is shown in Figure 4. From the snapshots of dislocation evolution, it can be found that a dislocation with Burgers vector of $\vec{b} = [101]/2$ nucleates at the corner of a metal layer with a stacking fault left behind (Figure 4b) and then slip in the $\{111\}$ slip plane (Figure 4c). We found that the onset of plasticity corresponds to the emission of $\{111\}\langle 112\rangle$ leading partial dislocations from the sharp corner where the atoms have the higher energy [28,29]. Then, the trailing partial dislocation nucleates from same site (Figure 4d), following the leading partial dislocation, and is finally trapped by the graphene-metal interface. The dislocation process can be expressed as

$$\frac{1}{6}[2\bar{1}1] + \frac{1}{6}[112] \rightarrow \frac{1}{2}[101] \quad (2)$$

However, the leading partial dislocation moving along the slip surface is eventually pinned near the interface but never penetrates beyond the single layer of graphene due to the strong C-C bond network of the graphene. This observation is consistent with the pile-up of dislocations at the graphene

interface observed in Kim's experiments [8]. For nano-twined metal nanowires, the transmission of dislocations through coherent twin boundaries (CTBs) was observed in the strain-softening stage [30]. However, when the dislocation reaches the interface of Ni and graphene, no penetration of the dislocation across the interface is observed. That means that graphene can hinder the movement of dislocation more efficiently than CTBs.

Figure 5 shows typical dislocation behaviors in CCS nanolayered composite nanowire. At the onset of plasticity, dislocation nucleates at the sharp edge in the surface, and then propagates cross the nanowire section. With the strain over 12.5%, the dislocations pile-up is observed in the metal layer, as shown in Figure 5e and Figure 5f, which suggests the flow stress of metal matrix could possibly be enhanced by inclusion of graphene sheets.

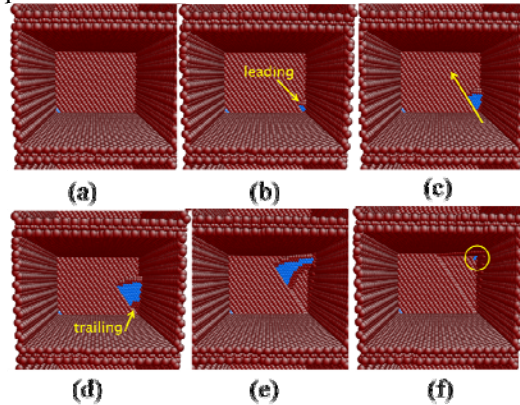


Figure 4. Snapshots of dislocation in SCS composites nanowires with the interlayer distance of 6.0 nm ($T=10$ K) under compressive loading at the initial yielding. (a) The dislocation nucleates from the corner. (b) The leading partial dislocation emission. (c) The leading partial dislocation slips along the slip plane. (d) The trailing partial dislocation nucleates at the same corner. (e) The leading and trailing dislocation move together across the nanolayer. (f) The dislocation is finally trapped by graphene-metal interface. For clarity, the front surface and perfect FCC atoms are not shown. Atoms are colored according to common neighbour analysis (CNA) [31].

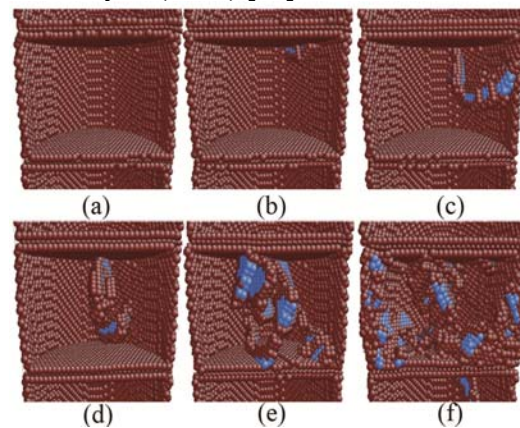


Figure 5. Snapshots of dislocation in CCS composites nanowires with the interlayer distance of 6.0 nm. (a) Stress-free state. Dislocation nucleates at the nanowire surface (b) and then propagates cross the nanowire from (c) to (d). With the compressive loading increasing, the dislocation pile-up (e) and (f) can be observed in the metal layer.

3.3 Temperature effects on the yield stress

In addition, the compressive mechanical behaviors of SCS nanowires are simulated at different temperatures (temperature varies between 10K and 400 K). According to the desired temperature, the initial velocities are assigned to atoms in the model with using Maxwell-Boltzmann distribution and then the model is subjected to compressive loading. The typical stress-strain curves for SCS nanolayered nanowires at different temperatures are shown in Figure 6a. According to this figure, the

Young's modulus decrease monotonically with temperature. Figure 6b shows the temperature dependence of yield stress for the SCS nanowires and CCS nanowires. The similar temperature dependence was also observed in single crystalline Cu nanowires [29] and Ni nanowires [32]. With the temperature increasing, the equilibrium distance of the atoms separation is increased, which causes the elastic modulus of nanowires to be reduced [32]. In addition, the temperature dependence of nucleation stress is determined by the small activation volume related to surface sources. The nucleation stress can be written as [33]

$$\sigma = \frac{Q^*}{\hat{\Omega}} - \frac{k_B T}{\hat{\Omega}} \ln \frac{k_B T N \nu_0}{E \dot{\epsilon} \hat{\Omega}} \quad (3)$$

in which, the first term $Q^*/\hat{\Omega}$ is the athermal nucleation stress, and the prefactor of the second term $k_B T/\hat{\Omega}$ has a stress unit, and it sets the scale of nucleation stress reduction due to thermal fluctuation.

The ratio between $k_B T N \nu_0$ and $E \dot{\epsilon} \hat{\Omega}$ determined the competition of thermal and mechanical effects in mediating the nucleation stress reduction due to thermal fluctuations. So the nucleation stress scales with $\ln T$, and the nucleation stress should be most sensitive to temperature, particularly when the activation volume is small. With temperature increasing, the dislocation nucleation takes place more rapidly at a higher temperature, which leads to the yield stress decreasing with temperature increasing.

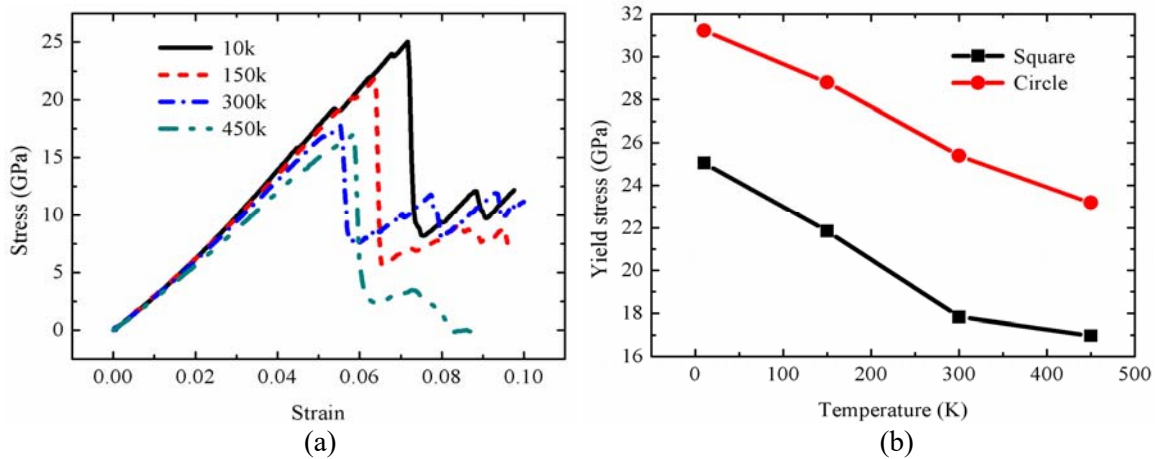


Figure 6. (a) Compressive stress-strain curves for the SCS nanowire at different temperatures with interlayer distance of about 6 nm. (b) The yielded stress as a function of temperature of SCS nanowires and CSC nanowires.

4. Conclusions

In this work, we study the compressive behaviors of the graphene/Ni nanolayered composite nanowires with both square and circular cross-sections by using molecular dynamics simulations. The results show that the stress for dislocation nucleation is low in SCS composite nanowires, thus the yield stress of SCS composite nanowires is dependent on the interlayer distance of graphene sheets. But stress for dislocation nucleation is high for CCS composite nanowires, with no obvious strengthening effect by graphene observed. For metal layers with relative low dislocation nucleation stress, graphene can be used as an impermeable interface to hinder the motion of dislocation. In addition, the strong temperature dependent yield stress is observed in all nanolayered composite nanowires. Graphene is an effective barrier against dislocation motion in nanolayered composites and the present results are expected to contribute to the design of novel metal matrix nanocomposites enhanced by graphene.

Acknowledgments

The authors thank the supports from the National Natural Science Foundation of China (11272300, 11272030 and 11472025), the Fundamental Research Funds for the Central Universities and the Beijing higher Education Young Elite Teacher Project.

References

- [1] A.K. Geim and K.S. Novoselov. The rise of graphene. *Nature Material*, 6: 183-191,2007.
- [2] C. Lee, X. Wei, J.W. Kysar and J. Hone. Measurement of the elastic properties and intrinsic strength of monolayer graphene. *Science*, 321:385-388, 2008.
- [3] J.R. Williams, L. DiCarlo and C.M. Marcus. Quantum hall effect in a gate-controlled p-n junction of graphene. *Science*, 317:638-641, 2007.
- [4] I.A. Ovid'Ko. Metal-graphene nanocomposites with enhanced mechanical properties: a review. *Reviews on Advanced Materials Science*, 38: 190-200,2014.
- [5] D. Kuang, L. Xu, L. Liu, W. Hu and Y. Wu. Graphene-nickel composites. *Applied Surface Science*, 273: 484-490, 2013.
- [6] M. Lee, L. Lee, S. Kim, H. Lee, J. Park, K.H. Choi, H.K. Kim, D.G. Kim, D.Y. Lee, S.W. Nam and J.U. Park. High-performance, transparent and stretchable electrodes using graphene-metal nanowire hybrid structures. *Nano Letter*, 13: 2814-2821, 2013.
- [7] J. Wang, Z. Li, G. Fan, H. Pan, Z. Chen and D. Zhang. Reinforcement with graphene nanosheets in aluminum matrix composites. *Scripta Materialia*, 66: 594-597, 2012.
- [8] Y. Kim, J. Lee, M.S. Yeom, J.W. Shin H. Kim, Y. Cui, J.W. Kysar, J. Hone, Y. Jung, S.J. Seung and M Han. Strengthening effect of single-atomic-layer graphene in metal-graphene nanolayered composites. *Nature Communications*, 4: 2114-2120, 2013.
- [9] J. Hwang, T. Yoon, S.H. Jin, J. Lee, T.S. Kim, S.H. Hong and S. Jeon. Enhanced Mechanical Properties of Graphene/Copper Nanocomposites Using a Molecular-Level Mixing Process. *Advanced Material*, 25: 6724-6729, 2013.
- [10] S. Chang, A.K. Nair and M.J. Buehler. Nanoindentation study of size effects in nickel -graphene nanocomposites. *Philosophical Magazine Letters*, 93: 196-203, 2013.
- [11] X.Y. Liu, F.C. Wang, H.A. Wu and W.Q. Wang. Strengthening metal nanolaminates under shock compression through dual effect of strong and weak graphene interface. *Applied Physical Letters*, 104: 231901, 2014.
- [12] I.A. Ovid'Ko and A.G. Sheinerman. Competition between plastic deformation and fracture processes in metal-graphene layered composites. *Journal of Physics D: Applied Physics*, 47: 495302, 2014.
- [13] H. Huang, X.B. Tang, F.D. Chen, Y.H Yang, J. Liu, H. Li and D. Chen. Radiation damage resistance and interface stability of copper-graphene nanolayered composite. *Journal of Nuclear Materials*, 460, 16-22, 2015.
- [14] A. Misra, J.P. Hirth and R.G. Hoagland. Length-scale-dependent deformation mechanisms in incoherent metallic multilayered composites. *Acta Materialia*, 53: 4817-4824, 2005.
- [15] J. Wang and A. Misra. An overview of interface-dominated deformation mechanisms in metallic multilayers. *Current Opinion in Solid State and Materials Science*, 15: 20-28, 2011.
- [16] X.H. Shi, Q.F. Yin and Y.J. Wei. A theoretical analysis of the surface dependent binding, peeling and folding of graphene on single crystal copper. *Carbon*, 50: 3055-3063, 2012.
- [17] S. Plimpton. Fast Parallel Algorithms for Short-Range Molecular Dynamics. *Journal of Computational Physics*, 117: 1-19, 1995.
- [18] D. Farkas, M.J. Mehl and D.A. Papaconstantopoulos. Interatomic potentials for monoatomic metals from experimental data and ab initio calculations. *Physical Review B*, 59: 3393, 1999.
- [19] S.J. Stuart, A.B. Tutein and J.A. Harrison. A reactive potential for hydrocarbons with intermolecular interactions. *Journal of Chemical Physics*, 112: 6472, 2000.
- [20] S. Huang, D.S. Mainardi and P.B. Balbuena. Structure and dynamics of graphite-supported nanoclusters. *Surface Science*, 545: 163-179, 2003.

- [21] S. Nosé. A unified formulation of the constant temperature molecular dynamics methods. *Journal of Chemical Physics*, 81: 511, 1984.
- [22] L.Verlet. Computer "experiments" on classical fluids. *Physical Review*, 159: 98-103, 1967.
- [23] M. Zhou. A new look at the atomic level virial stress: On continuum-molecular system equivalence, *Proceedings of the Royal Society A: Mathematical, Physical and Engineering Sciences*, 459: 2347-2392, 2003.
- [24] J. Li. AtomEye: An efficient atomistic configuration viewer. *Modelling and Simulation in Materials Science and Engineering*, 11: 173, 2003.
- [25] Y.F. Zhang and H.C. Huang. Do Twin Boundaries Always Strengthen Metal Nanowires? *Nanoscale Research Letters*, 4: 34-38, 2009.
- [26] E.O. Hall. The deformation and ageing of mild steel: III discussion of results. *Proceedings of the Physical Society Section B*, 64: 747-753, 1951.
- [27] N.J. Petch. The cleavage strength of polycrystals. *Journal of the Iron and Steel Institute*, 174: 25-28, 1953.
- [28] Z.Y. Yang, Z.X. Lu and Y.P. Zhao. Shape effects on the yield stress and deformation of silicon nanowires: A molecular dynamics simulation. *Journal of Applied Physics*, 106: 023537, 2009.
- [29] A. Cao and E. Ma. Sample shape and temperature strongly influence the yield strength of metallic nanopillars. *Acta Materialia*, 56: 4816-4828, 2008.
- [30] C. Deng and F. Sansoz. Fundamental differences in the plasticity of periodically twinned nanowires in Au, Ag, Al, Cu, Pb and Ni. *Acta Materialia*, 57: 6090-6101, 2009.
- [31] D. Li, F.C. Wang, Z.Y. Yang and Y.-P. Zhao. How to identify dislocations in molecular dynamics simulations? *Science China-Physics Mechanics and Astronomy*, 57(12): 2177-2187, 2014.
- [32] A.R. Setoodeh, H. Attariani and M. Khosrownejad. Nickel nanowires under uniaxial loads: A molecular dynamics simulation study. *Computational Material Sciences*, 44: 378-384, 2008.